hep-ph/0405192

Two-loop gluino corrections to the inclusive $B \to X_s\gamma$ decay in CP violating MSSM with large $\tan\beta$

Tai-Fu Feng

Department of Physics, 40014 University of Jyväskylä,Finland

(Dated: February 1, 2008)

Abstract

We investigate two-loop gluino corrections to the effective Lagrangian for $b \to s + \gamma(g)$ in the minimal supersymmetric extension of the standard model (MSSM) at large $\tan\beta$, including the contributions in which quark flavor change is mediated by charginos. Using the translation invariant of loop momenta and the Ward-Takahashi identities (WTIs) that are required by the $SU(3)_c \times U(1)_{em}$ gauge invariance, we simplify our expressions to concise forms. As an example, we discuss two-loop gluino corrections to the CP asymmetry of inclusive $B \to X_s\gamma$ decay in CP violating MSSM.

PACS numbers: 11.30.Er, 12.60.Jv,14.80.Cp

Keywords: two-loop, inclusive decay, supersymmetry

I. INTRODUCTION

The measurements of the branching ratios at CLEO, ALEPH and BELLE [1] give the combined result

$$BR(B \to X_s\gamma) = (3.11 \pm 0.42 \pm 0.21) \times 10^{-4} \;, \tag{1}$$

which agrees with the next-to-leading order (NLO) standard model (SM) prediction [2]

$$BR(B \to X_s\gamma) = (3.29 \pm 0.33) \times 10^{-4} \;. \tag{2}$$

Good agreement between the experiment and the theoretical prediction of the SM implies that the new physics scale should lie well above the electroweak (EW) scale. The systematic analysis of new physics corrections to $B \to X_s\gamma$ up to two-loop order can help us understanding where the new physics scale sets in, and the distribution of new physical particle masses around this scale. In principle, the two-loop corrections can be large when some additional parameters are involved at this perturbation order beside the parameters appearing in one loop results. In other words, including the two-loop contributions one can obtain a more exact constraint on the new physics parameter space from the present experimental results.

Beside the Cabibbo-Kobayashi-Maskawa (CKM) mechanism, the soft breaking terms provide a new source of CP and flavor violation in the MSSM. Those CP violating phases can affect the important observables in the mixing of Higgs bosons [3], the lepton and neutron's electric dipole moments (EDMs) [4, 5], lepton polarization asymmetries in the semi-leptonic decays [6], the production of P-wave charmonium and bottomonium [7], and CP violation in rare B-decays and in $B^0\bar{B}^0$ mixing [8]. At present, the strictest constraints on those CP violation phases originate from the lepton and neutron's EDMs. Nevertheless, if we invoke a cancellation mechanism among different supersymmetric contributions [4], or choose the sfermions of the first generation heavy enough [5], the loop inducing lepton and neutron's EDMs bound the argument of the μ parameter to be $\leq \pi/(5\tan\beta)$, leaving no constraints on the other explicitly CP violating phases.

The supersymmetry models at large $\tan\beta$ are implied by grand unified theories, where the unification of up- and down-type quark Yukawa couplings is made [9]. From the technical viewpoint, the dominant contributions to the relevant effective Lagrangian are the terms proportional to $(\tan\beta)^n$ $(n = 1,\ 2, \cdots)$ in a large $\tan\beta$ scenario. This will simplify our

two-loop analysis drastically since we just keep those terms enhanced by $\tan\beta$.

Assuming no additional sources of flavor violation other than the CKM matrix elements, the authors of [10] present an exact analysis of the two-loop gluino corrections to the rare decay $b \to s + \gamma(g)$ in which quark flavor change is mediated by the charged Higgs in CP conserving MSSM at large $\tan\beta$. They also compare their exact result with that originating from the heavy mass expansion (HME) approximation [11]. Although the HME result approximates the exact two-loop analysis adequately when the supersymmetry energy scale is high enough, their analysis implies that the difference between the HME approximation and exact calculation is obvious in some parameter space of the MSSM. However, they do not consider the case in which quark flavor change is mediated by the charginos (the super partners of the charged Higgs and W bosons). In fact, we cannot provide any strong reason to ignore the contribution from the diagrams in which quark flavor change is induced by the charginos, even within large $\tan\beta$ scenarios. In this work, we present a complete analysis on the two-loop gluino corrections to the rare transitions $b \to s + \gamma(g)$ by including the contributions of those diagrams where quark flavor change is mediated by charginos in the framework of CP violating MSSM at large $\tan\beta$. Furthermore, we also simplify our expressions to concise forms through loop momentum invariant and the WTIs that are required by the $SU(3)_c \times U(1)_{em}$ gauge invariance.

The paper is organized as follows. In Sec. II, we give all the diagrams needed to evaluate the $O(\alpha_s \tan\beta)$ contributions to the Wilson coefficients C_7 and C_8 entering the branching ratio $BR(B \to X_s\gamma)$. The corresponding Wilson coefficients at the matching EW scale $\mu_{\rm EW}$ are also presented there. We apply the effective Lagrangian to the rare decay $B \to X_s\gamma$ in Sec. III. By the numerical method, we show the two-loop corrections on the CP asymmetry for the process. Our conclusion is given in Sec. IV, and some long formulae are collected in appendices.

II. THE WILSON COEFFICIENTS FROM THE TWO-LOOP DIAGRAMS

In this section, we derive the relevant Wilson coefficients for the partonic decay $b \to s\gamma$ including two-loop gluino corrections. In a conventional form, the effective Hamilton is

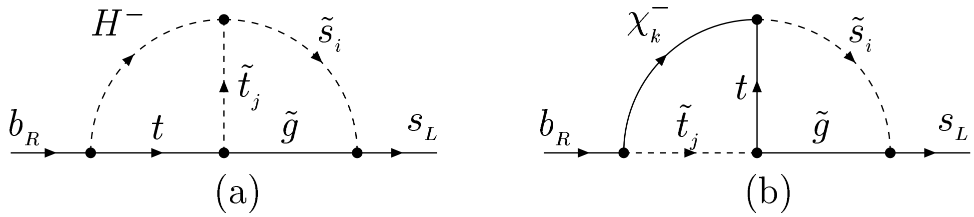

FIG. 1: The self energy diagrams which lead to the magnetic and chromo-magnetic operators in the MSSM, the corresponding triangle diagrams are obtained by attaching a photon or gluon in all possible ways.

written as

$$H_{eff} = -\frac{4G_F}{\sqrt{2}} V_{ts}^* V_{tb} \sum_{i=1}^{8} C_i(\mu)\mathcal{O}_i \ , \tag{3}$$

where V is the CKM matrix. The definitions of the magnetic and chromo-magnetic dipole operators are

$$\begin{aligned} \mathcal{O}_7 &= \frac{e}{(4\pi)^2} m_b(\mu) \bar{s}_L \sigma^{\mu\nu} b_R F_{\mu\nu} \ , \\ \mathcal{O}_8 &= \frac{g_s}{(4\pi)^2} m_b(\mu) \bar{s}_L T^a \sigma^{\mu\nu} b_R G^a_{\mu\nu} \ , \end{aligned} \tag{4}$$

where $F_{\mu\nu}$ and $G^a_{\mu\nu}$ are the field strengths of the photon and gluon respectively, and T^a ($a = 1, \cdots, 8$) are $SU(3)_c$ generators. In addition, e and g_s represent the EW and strong couplings respectively. The other operators $\mathcal{O}_i$ ($i = 1, \cdots, 6$) are defined in [12].

In the framework of CP violation MSSM, the one-loop analysis on the CP asymmetry of inclusive $B \to X_s\gamma$ decay has been presented elsewhere [9]. The two loop gluino diagrams, contributing at $\mathcal{O}(\alpha_s \tan\beta)$ to the Wilson coefficients of the magnetic and chromo-magnetic dipole operators, are obtained from the self energy diagrams (a), (b) of FIG. 1 by attaching a photon or gluon in all possible ways. The calculation of the Wilson coefficients for the operators in Eq. (4) at the two loop order is more challenging than that at the one loop order. Before we give those Wilson coefficient expressions explicitly, we state firstly the concrete steps required to obtain the coefficients from those two loop diagrams.

- After writing the amplitudes of those two loop triangle diagrams, we expand them in powers of external momenta to the second order.

- The even rank tensors in the loop momenta q_1, q_2 can be replaced as follows

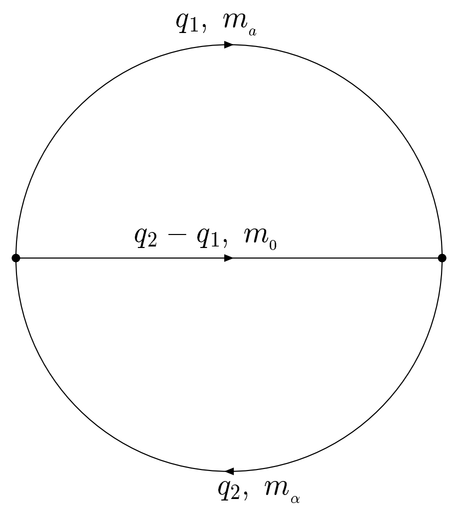

FIG. 2: The two-loop vacuum diagram with momenta and masses as in Eq. 5.

$$\begin{aligned}
&\int\frac{d^Dq_1}{(2\pi)^D}\frac{d^Dq_2}{(2\pi)^D}\frac{q_{1\mu}q_{1\nu},\ q_{1\mu}q_{2\nu}}{\mathcal{D}_{_0}}\longrightarrow\frac{g_{\mu\nu}}{D}\int\frac{d^Dq_1}{(2\pi)^D}\frac{d^Dq_2}{(2\pi)^D}\frac{q_1^2,\ q_1\cdot q_2}{\mathcal{D}_{_0}}\;,\\
&\int\frac{d^Dq_1}{(2\pi)^D}\frac{d^Dq_2}{(2\pi)^D}\frac{q_{1\mu}q_{1\nu}q_{1\rho}q_{1\sigma},\ q_{1\mu}q_{1\nu}q_{1\rho}q_{2\sigma}}{\mathcal{D}_{_0}}\\
&\longrightarrow\frac{T_{_{\mu\nu\rho\sigma}}}{D(D+2)}\int\frac{d^Dq_1}{(2\pi)^D}\frac{d^Dq_2}{(2\pi)^D}\frac{q_1^4,\ q_1^2(q_1\cdot q_2)}{\mathcal{D}_{_0}}\;,\\
&\int\frac{d^Dq_1}{(2\pi)^D}\frac{d^Dq_2}{(2\pi)^D}\frac{q_{1\mu}q_{1\nu}q_{2\rho}q_{2\sigma}}{\mathcal{D}_{_0}}\\
&\longrightarrow\int\frac{d^Dq_1}{(2\pi)^D}\frac{d^Dq_2}{(2\pi)^D}\frac{1}{\mathcal{D}_{_0}}\Big(\frac{D(q_1\cdot q_2)^2-q_1^2q_2^2}{D(D-1)(D+2)}T_{_{\mu\nu\rho\sigma}}-\frac{(q_1\cdot q_2)^2-q_1^2q_2^2}{D(D-1)}g_{\mu\nu}g_{\rho\sigma}\Big)\;, \qquad (5)
\end{aligned}$$

where D is the time-space dimension, $T_{_{\mu\nu\rho\sigma}}=g_{\mu\nu}g_{\rho\sigma}+g_{\mu\rho}g_{\nu\sigma}+g_{\mu\sigma}g_{\rho\nu}$ and $\mathcal{D}_{_0}=((q_2-q_1)^2-m_{_0}^2)(q_1^2-m_{_a}^2)(q_2^2-m_{_\alpha}^2)$. The odd rank tensors in the loop momenta can be dropped since the integrations are symmetric under the transformation $q_{1,2}\to-q_{1,2}$. Here, we only retain the simplest two-loop propagator composition $1/\mathcal{D}_{_0}$ which corresponds to the two-loop vacuum diagram (FIG. 2). Any complicated composition of two-loop propagators can be expressed as the linear combination of the simplest one $1/\mathcal{D}_{_0}$ by use of the obvious decomposition formula

$$\frac{1}{(Q^2-m_{_A}^2)(Q^2-m_{_B}^2)}=\frac{1}{m_{_A}^2-m_{_B}^2}\Big(\frac{1}{Q^2-m_{_A}^2}-\frac{1}{Q^2-m_{_B}^2}\Big)\;, \qquad (6)$$

with $Q=q_1,\ q_2$, or q_2-q_1. As an example, we apply the above two steps to the triangle diagram in which a external photon is attached to the internal squark $\tilde{s}_{_i}$ line (FIG. 3). After expanding the corresponding amplitude in powers of external momenta to the second order, we have

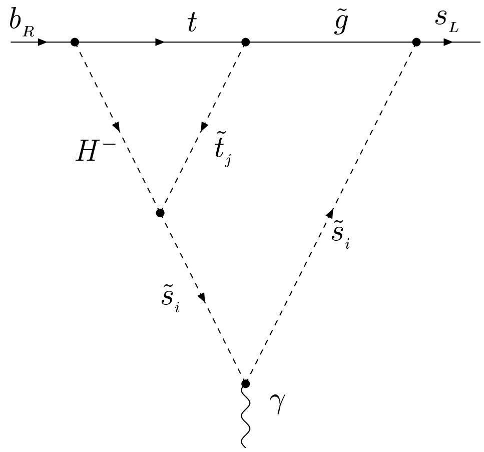

FIG. 3: A triangle diagram in which the external photon is attached to squark $\tilde{s}_i$.

$$
\begin{aligned}
iA^{\gamma}_{\mu}(p,k) =& -i\frac{4}{3}e_d g_s^2 \frac{e^3}{m_{\rm w} s_{\rm w}^2} V^*_{ts} V_{tb} (\frac{m_b}{m_{\rm w}} \tan\beta)(\mathcal{Z}_{\tilde{s}})_{2,i} (\mathcal{Z}^{\dagger}_{\tilde{s}})_{i,2} (|\mu| m_t e^{-i\theta_\mu} (\mathcal{Z}_{\tilde{t}})_{2,j} \\
&+ \frac{\sqrt{2} m_{\rm w} s_{\rm w} \mathbf{A}_s}{e} (\mathcal{Z}_{\tilde{t}})_{1,j}) \int \frac{d^D q_1}{(2\pi)^D} \frac{d^D q_2}{(2\pi)^D} \frac{1}{\mathcal{D}_H (q_1^2 - m^2_{\tilde{s}_i})} \\
&\times \Big\{ 1 + \frac{2q_1 \cdot (2p+k)}{q_1^2 - m^2_{\tilde{s}_i}} + \frac{2q_2 \cdot p}{q_2^2 - m^2_{H^+}} \Big\} \\
&\times \Big\{ (\mathcal{Z}^{\dagger}_{\tilde{t}})_{j,3} \not{q}_1 \not{q}_2 (2q_1 - 2p - k)_\mu \omega_+ \\
&- m_t |m_3| e^{i\theta_3} (\mathcal{Z}^{\dagger}_{\tilde{t}})_{j,2} (2q_1 - 2p - k)_\mu \omega_+ \Big\} ,
\end{aligned} \tag{7}
$$

where $p,\ k$ represent the incoming momenta of the external quark b and photon respectively, $\mathcal{D}_H = ((q_2-q_1)^2 - m^2_{\tilde{t}_j})(q_1^2 - |m_3|^2)(q_1^2 - m^2_{\tilde{s}_i})(q_2^2 - m_t^2)(q_2^2 - m^2_{H^+})$ $(i,\ j = 1,\ 2)$ and $e_d = -1/3$. $\mathcal{Z}_{\tilde{q}}$ $(q = u,\ d,\ \cdots,\ t)$ are the mixing matrices of scalar quarks, and $\mathbf{A}_q$ are the corresponding trilinear soft breaking parameters. Furthermore, $\theta_{3,\mu}$ denote the CP phases of the $SU(3)_c$ gaugino mass and of the μ parameter respectively. Since the quark mass m_b from the Yukawa coupling of bottom quark is same order as the external momenta $p,\ k$ in magnitude, we just expand the propagators in powers of the external momenta to the first order. In the soft breaking potential, the CP phase θ_3 is contained in the gluino mass terms

$$
|m_3| e^{i\theta_3} \lambda_G \lambda_G + |m_3| e^{-i\theta_3} \overline{\lambda}_G \overline{\lambda}_G \ , \tag{8}
$$

where λ_G denotes the gluino in a two-component Majorana spinor. With the redefini-

tion of the gluino field

$$\lambda_{_G} \to \lambda_{_G} e^{-\frac{i}{2}\theta_3}\ ,$$
$$\overline{\lambda}_{_G} \to \overline{\lambda}_{_G} e^{\frac{i}{2}\theta_3}\ , \tag{9}$$

the mass terms are transformed into

$$|m_{_3}|\overline{\tilde{g}}\tilde{g} \tag{10}$$

with the four-component Majorana spinor

$$\tilde{g} = \begin{pmatrix} \lambda_{_G} \\ \overline{\lambda}_{_G} \end{pmatrix}\ . \tag{11}$$

Correspondingly, the CP phase $\theta_{_3}$ is transfered from the mass terms to the quark-squark-gluino vertex which is given by [13]

$$-\mathcal{L}_{_{\tilde{q}q\tilde{g}}} = \sqrt{2} g_{_s} T^a_{\alpha\beta} \sum_q \Big[- e^{-\frac{i}{2}\theta_3} (\mathcal{Z}_{_{\tilde{q}}})_{_{2,i}} \overline{q}^\alpha \omega_- \tilde{g}_a \tilde{q}^\beta_{_i}$$
$$+ e^{\frac{i}{2}\theta_3} (\mathcal{Z}_{_{\tilde{q}}})_{_{1,i}} \overline{q}^\alpha \omega_+ \tilde{g}_a \tilde{q}^\beta_{_i} \Big] + \text{H.c.} \tag{12}$$

Here, $\alpha,\ \beta = 1,\ 2,\ 3$ are quark and squark color indices, and $\omega_\pm = \frac{1\pm\gamma_5}{2}$. This is the reason why there is a $|m_{_3}|$ rather than $m_{_3}$ in the gluino propagator. Using Eq. 5 and Eq. 6, the amplitude of FIG. 3 is finally formulated as

$$iA^\gamma_\mu(p,k) = -i\frac{4}{3} e_{_d} g^2_{_s} \frac{e^3}{m_{_\mathrm{w}} s^2_{_\mathrm{w}}} V^*_{_{ts}} V_{_{tb}} (\frac{m_{_b}}{m_{_\mathrm{w}}} \tan\beta) (\mathcal{Z}_{_{\tilde{s}}})_{_{2,i}} (\mathcal{Z}^\dagger_{_{\tilde{s}}})_{_{i,2}} (|\mu| m_{_t} e^{-i\theta_\mu} (\mathcal{Z}_{_{\tilde{t}}})_{_{2,j}}$$
$$+ \frac{\sqrt{2} m_{_\mathrm{w}} s_{_\mathrm{w}} \mathbf{A}_{_s}}{e} (\mathcal{Z}_{_{\tilde{t}}})_{_{1,j}}) \int \frac{d^D q_1}{(2\pi)^D} \frac{d^D q_2}{(2\pi)^D} \frac{1}{\mathcal{D}_{_H} (q^2_1 - m^2_{_{\tilde{s}_i}})}$$
$$\times \Big\{ (\mathcal{Z}^\dagger_{_{\tilde{t}}})_{_{j,3}} \Big[\frac{4}{D} \frac{q^2_1 q_1 \cdot q_2}{q^2_1 - m^2_{_{\tilde{s}_i}}}\ (2p+k)_\mu \omega_+ - q_1 \cdot q_2\ (2p+k)_\mu \omega_+$$
$$+ \frac{4}{q^2_2 - m^2_{_{H^+}}} \Big(\frac{D(q_1 \cdot q_2)^2 - q^2_1 q^2_2}{D(D-1)}\ p_\mu \omega_+ - \frac{(q_1 \cdot q_2)^2 - q^2_1 q^2_2}{D(D-1)}\ \gamma_\mu \not{p} \omega_+ \Big) \Big]$$
$$- m_{_t} |m_{_3}| e^{i\theta_3} (\mathcal{Z}^\dagger_{_{\tilde{t}}})_{_{j,2}} \Big[\frac{4}{D} \frac{q^2_1}{q^2_1 - m^2_{_{\tilde{s}_i}}}\ (2p+k)_\mu \omega_+ + \frac{4}{D} \frac{q_1 \cdot q_2}{q^2_2 - m^2_{_{H^+}}}\ p_\mu \omega_+$$
$$- (2p+k)_\mu \omega_+ \Big] \Big\}\ . \tag{13}$$

In a similar way, we can obtain the other triangle diagram amplitudes.

- Using loop momentum translation invariant, we formulate the sum of those amplitudes in gauge invariance form explicitly, then extract the corresponding Wilson coefficients which are expressed by the two-loop vacuum integrals [14]. In fact, there are many identities among those two-loop integrations. In order to obtain those necessary identities which are used to simplify the sum of those triangle amplitudes, we start from the zero integration such as

$$\int \frac{d^Dq_1}{(2\pi)^D}\frac{d^Dq_2}{(2\pi)^D}\frac{q_1\cdot p\,\not q_1(\not q_2-\not q_1)}{\mathcal{D}_{_0}}\equiv 0\;. \tag{14}$$

Under the loop momentum translation $q_2\rightarrow q_2-a$ where a is same order as the external momentum p in magnitude, we expand the integration in powers of the momenta $p,\ a$ to the second order

$$\begin{aligned}
&\int \frac{d^Dq_1}{(2\pi)^D}\frac{d^Dq_2}{(2\pi)^D}\frac{q_1\cdot p}{\mathcal{D}_{_0}}\not q_1(\not q_2-\not q_1)\\
&=\int \frac{d^Dq_1}{(2\pi)^D}\frac{d^Dq_2}{(2\pi)^D}\frac{q_1\cdot p}{\mathcal{D}_{_0}}\Big\{1+\frac{2(q_2-q_1)\cdot a}{(q_2-q_1)^2-m_{_0}^2}+\frac{2q_2\cdot a}{q_2^2-m_{_\alpha}^2}\Big\}\\
&\times\Big\{\not q_1(\not q_2-\not q_1)-\not q_1\not a\Big\}\\
&=\int \frac{d^Dq_1}{(2\pi)^D}\frac{d^Dq_2}{(2\pi)^D}\frac{1}{\mathcal{D}_{_0}}\Big\{-\frac{q_1^2}{D}\not p\not a+\frac{2}{(q_2-q_1)^2-m_{_0}^2}\Big[\Big(\frac{D(q_1\cdot q_2)^2-q_1^2q_2^2}{D(D-1)}\\
&+\frac{q_1^4-2q_1^2q_1\cdot q_2}{D}\Big)(p\cdot a)-\frac{(q_1\cdot q_2)^2-q_1^2q_2^2}{D(D-1)}(\not p\not a)\Big]\\
&+\frac{2}{q_2^2-m_{_\alpha}^2}\Big[\Big(\frac{D(q_1\cdot q_2)^2-q_1^2q_2^2}{D(D-1)}-\frac{q_1^2q_1\cdot q_2}{D}\Big)(p\cdot a)\\
&-\frac{(q_1\cdot q_2)^2-q_1^2q_2^2}{D(D-1)}(\not p\not a)\Big]\Big\}\equiv 0\;.
\end{aligned}\tag{15}$$

The above identical equation implies

$$\begin{aligned}
&\int \frac{d^Dq_1}{(2\pi)^D}\frac{d^Dq_2}{(2\pi)^D}\frac{1}{\mathcal{D}_{_0}}\Big\{\frac{1}{(q_2-q_1)^2-m_{_0}^2}\Big[\frac{D(q_1\cdot q_2)^2-q_1^2q_2^2}{D(D-1)}+\frac{q_1^4-2q_1^2q_1\cdot q_2}{D}\Big]\\
&+\frac{1}{q_2^2-m_{_\alpha}^2}\Big[\frac{D(q_1\cdot q_2)^2-q_1^2q_2^2}{D(D-1)}-\frac{q_1^2q_1\cdot q_2}{D}\Big]\Big\}\equiv 0\;,\\
&\int \frac{d^Dq_1}{(2\pi)^D}\frac{d^Dq_2}{(2\pi)^D}\frac{1}{\mathcal{D}_{_0}}\Big\{\frac{2}{(q_2-q_1)^2-m_{_0}^2}\frac{(q_1\cdot q_2)^2-q_1^2q_2^2}{D(D-1)}\\
&+\frac{2}{q_2^2-m_{_\alpha}^2}\frac{(q_1\cdot q_2)^2-q_1^2q_2^2}{D(D-1)}+\frac{q_1^2}{D}\Big\}\equiv 0\;.
\end{aligned}\tag{16}$$

Similarly, we can get the following identities from the invariant of Eq. 14 under the loop momentum translation $q_1\rightarrow q_1-a,\ q_2\rightarrow q_2-a$:

$$\int \frac{d^Dq_1}{(2\pi)^D}\frac{d^Dq_2}{(2\pi)^D}\frac{1}{\mathcal{D}_{_0}}\Big\{-\frac{2+D}{D}q_1\cdot(q_2-q_1)+\frac{2}{q_1^2-m_{_a}^2}\frac{q_1^2q_1\cdot(q_2-q_1)}{D}$$

$$+\frac{2}{q_2^2-m_{\alpha}^2}\Big[\frac{D(q_1\cdot q_2)^2-q_1^2q_2^2}{D(D-1)}-\frac{q_1^2q_1\cdot q_2}{D}\Big]\Big\}\equiv 0\;,$$

$$\int\frac{d^Dq_1}{(2\pi)^D}\frac{d^Dq_2}{(2\pi)^D}\frac{1}{\mathcal{D}_{0}}\Big\{\frac{q_1\cdot(q_2-q_1)}{D}-\frac{2}{q_2^2-m_{\alpha}^2}\frac{(q_1\cdot q_2)^2-q_1^2q_2^2}{D(D-1)}\Big\}\equiv 0\;. \qquad (17)$$

Using the concrete expressions of two-loop vacuum integrals in Ref. [14], we can also verify those equations in Eq. 16 and Eq. 17 directly after some tedious calculations. Replacing the numerator of Eq. 14 with other odd rank tensors in the loop momenta $q_1,\ q_2$, the more additional identities among two-loop integrations are gotten. In general, those identities are linearly dependent. After some simplification, we obtain those linearly independent equations in appendix A. Certainly, those linearly independent equations can also be derived from those two-loop integrations in which the numerators are even rank tensors of the loop momenta $q_1,\ q_2$. However, the process to derive the linearly independent equations with the numerators in even powers of the loop momenta is more complicated than that with the numerators in odd powers of the loop momenta.

After the above procedure, we finally obtain the relevant coefficients from the charged Higgs contribution up to $\mathcal{O}(\alpha_{s}\tan\beta)$

$$\begin{aligned}C_{7,H}(\mu_{\rm w})=&\frac{8\sqrt{2}}{3}(4\pi)^3e_{d}(\alpha_{s}\tan\beta)(\mathcal{Z}_{\tilde s})_{2,i}(\mathcal{Z}_{\tilde s}^\dagger)_{i,2}\Big(|\mu|m_{t}e^{-i\theta_\mu}(\mathcal{Z}_{\tilde t})_{2,j}\\&+\frac{\sqrt{2}s_{\rm w}m_{\rm w}A_{s}}{e}(\mathcal{Z}_{\tilde t})_{1,j}\Big)\int\frac{d^4q_1}{(2\pi)^4}\frac{d^4q_2}{(2\pi)^4}\frac{1}{\mathcal{D}_{H}}\Big\{(\mathcal{Z}_{\tilde t}^\dagger)_{j,1}\mathcal{N}_{H(1)}^\gamma\\&-m_{t}|m_3|e^{i\theta_3}(\mathcal{Z}_{\tilde t}^\dagger)_{j,2}\mathcal{N}_{H(2)}^\gamma\Big\}\;,\\C_{8,H}(\mu_{\rm w})=&\frac{8\sqrt{2}}{3}(4\pi)^3(\alpha_{s}\tan\beta)(\mathcal{Z}_{\tilde s})_{2,i}(\mathcal{Z}_{\tilde s}^\dagger)_{i,2}\Big(|\mu|m_{t}e^{-i\theta_\mu}(\mathcal{Z}_{\tilde t})_{2,j}\\&+\frac{\sqrt{2}s_{\rm w}m_{\rm w}A_{s}}{e}(\mathcal{Z}_{\tilde t})_{1,j}\Big)\int\frac{d^4q_1}{(2\pi)^4}\frac{d^4q_2}{(2\pi)^4}\frac{1}{\mathcal{D}_{H}}\Big\{(\mathcal{Z}_{\tilde t}^\dagger)_{j,1}\mathcal{N}_{H(1)}^g\\&-m_{t}|m_3|e^{i\theta_3}(\mathcal{Z}_{\tilde t}^\dagger)_{j,2}\mathcal{N}_{H(2)}^g\Big\}\;,\end{aligned}\qquad (18)$$

where $\alpha_{s}=g_s^2/4\pi$, and the expressions of the form factors $\mathcal{N}_{H(1,2)}^{\gamma,\,g}$ can be found in appendix B. Note, Ref. [10] has also obtained the Wilson coefficients from the same diagrams. We formulate our expressions in the more concise forms using the identities from appendix A. For the chargino contribution that is ignored by Ref. [10], we can similarly have

$$
\begin{aligned}
C_{7,\chi_k}(\mu_{\rm w}) = & \frac{8\sqrt{2}}{3} e_d (4\pi)^3 \Big(\alpha_s \tan\beta\Big) (\mathcal{Z}_{\tilde{s}})_{2,i} (\mathcal{Z}^\dagger_{\tilde{s}})_{i,2} (\mathcal{Z}^\dagger_{\tilde{t}})_{j,1} (\mathcal{Z}^\dagger_{-})_{k,2} \\
& \times \int \frac{d^4q_1}{(2\pi)^4} \frac{d^4q_2}{(2\pi)^4} \frac{1}{\mathcal{D}_{\chi_k}} \Big\{ m_t m_{\chi_k} (\mathcal{Z}_{\tilde{t}})_{2,j} (\mathcal{Z}_+)_{2,k} \mathcal{N}^\gamma_{\chi^\pm_k(1)} \\
& + \sqrt{2} m_{\rm w} m_t (\mathcal{Z}_{\tilde{t}})_{2,j} (\mathcal{Z}_-)_{1,k} \mathcal{N}^\gamma_{\chi^\pm_k(2)} \\
& - \sqrt{2} m_{\rm w} |m_3| e^{i\theta_3} (\mathcal{Z}_{\tilde{t}})_{1,j} (\mathcal{Z}_-)_{1,k} \mathcal{N}^\gamma_{\chi^\pm_k(3)} \\
& + m_t^2 m_{\chi_k} |m_3| e^{i\theta_3} (\mathcal{Z}_{\tilde{t}})_{1,j} (\mathcal{Z}_+)_{2,k} \mathcal{N}^\gamma_{\chi^\pm_k(4)} \Big\} , \\
C_{8,\chi_k}(\mu_{\rm w}) = & \frac{8\sqrt{2}}{3} (4\pi)^3 \Big(\alpha_s \tan\beta\Big) (\mathcal{Z}_{\tilde{s}})_{2,i} (\mathcal{Z}^\dagger_{\tilde{s}})_{i,2} (\mathcal{Z}^\dagger_{\tilde{t}})_{j,1} (\mathcal{Z}^\dagger_{-})_{k,2} \\
& \times \int \frac{d^4q_1}{(2\pi)^4} \frac{d^4q_2}{(2\pi)^4} \frac{1}{\mathcal{D}_{\chi_k}} \Big\{ m_t m_{\chi_k} (\mathcal{Z}_{\tilde{t}})_{2,j} (\mathcal{Z}_+)_{2,k} \mathcal{N}^g_{\chi^\pm_k(1)} \\
& + \sqrt{2} m_{\rm w} m_t (\mathcal{Z}_{\tilde{t}})_{2,j} (\mathcal{Z}_-)_{1,k} \mathcal{N}^g_{\chi^\pm_k(2)} \\
& - \sqrt{2} m_{\rm w} |m_3| e^{i\theta_3} (\mathcal{Z}_{\tilde{t}})_{1,j} (\mathcal{Z}_-)_{1,k} \mathcal{N}^g_{\chi^\pm_k(3)} \\
& + m_t^2 m_{\chi_k} |m_3| e^{i\theta_3} (\mathcal{Z}_{\tilde{t}})_{1,j} (\mathcal{Z}_+)_{2,k} \mathcal{N}^g_{\chi^\pm_k(4)} \Big\} ,
\end{aligned}
\tag{19}
$$

with $\mathcal{D}_{\chi_k} = ((q_2-q_1)^2 - m_t^2)(q_1^2 - |m_3|^2)(q_1^2 - m^2_{\tilde{s}_i})(q_2^2 - m^2_{\tilde{t}_j})(q_2^2 - m^2_{\chi_k})$. $\mathcal{Z}_-$, $\mathcal{Z}_+$ are the left- and right-handed mixing matrices of charginos, and the form factors $\mathcal{N}^{\gamma,\,g}_{\chi^\pm_k(i)}$ $(i = 1,\ 2,\ 3,\ 4)$ are collected in appendix B. After we simplify the sum of the $\bar{s}b\gamma$ (g) triangle diagram amplitudes using the identities in appendix A, we find that the effective $\bar{s}b\gamma$ (g) vertices should also include the two-point operator

$$
\mathcal{O}_{\rm se} = \frac{1}{(4\pi)^2} m_b(\mu) \bar{s}_L (i\not{D})^2 b_R \ , \tag{20}
$$

beside the magnetic (chromo-magnetic) dipole operators $\mathcal{O}_7$ $(\mathcal{O}_8)$. Here, the covariant derivative acting on the quark fields is

$$
D_\mu = \partial_\mu - iee_q A_\mu - ig_s G_\mu , \tag{21}
$$

with $G_\mu = G^a_\mu T^a$. Certainly, the Wilson coefficient of this operator does not give any contribution to the rare process $b \to s\gamma$ after we evolve the corresponding coefficients from the matching EW scale to the hadronic scale. Nevertheless, when we extract the Wilson coefficients of $\mathcal{O}_7$ $(\mathcal{O}_8)$, it makes sense to keep this operator for the following reason. Beside the effective vertex with two quarks

$$
\mathcal{O}_{\rm se} \sim \frac{i}{(4\pi)^2} m_b p^2 \omega_+ \ , \tag{22}
$$

the operator $\mathcal{O}_{_{se}}$ can also induce the effective vertices with two quarks and one photon or gluon

$$\begin{aligned}
\mathcal{O}_{_{se}} &\sim \frac{i}{(4\pi)^2} ee_{_d} m_{_b}\Big(2p_{_\mu} + \not{k}\gamma_{_\mu}\Big)\omega_+ \;, \\
\mathcal{O}_{_{se}} &\sim \frac{i}{(4\pi)^2} g_{_s} T^a m_{_b}\Big(2p_{_\mu} + \not{k}\gamma_{_\mu}\Big)\omega_+
\end{aligned} \tag{23}$$

in the momentum space. Here, p, k are the incoming momenta of the external quark b and gauge boson (γ or g) respectively. For the effective $\bar{s}b\gamma$ (g) vertices $A_{_\mu}^{\gamma\,(g)}(p,k)$, the corresponding WTIs required by the $SU(3)_{_c} \times U(1)_{_{em}}$ gauge invariance are written as

$$\begin{aligned}
iee_{_d}\Big(\Sigma(p+k) - \Sigma(p)\Big) &= ik \cdot A^\gamma(p,k) \;, \\
ig_{_s}T^a\Big(\Sigma(p+k) - \Sigma(p)\Big) &= ik \cdot A^g(p,k) \;,
\end{aligned} \tag{24}$$

where $i\Sigma(p)$ represents the sum of amplitudes for the self energy diagrams (FIG. 1). Expanding the self energy amplitudes in powers of external momentum to the third order, we have

$$i\Sigma(p) = \frac{i}{(4\pi)^2} B_{_0} m_{_b} p^2 \;, \tag{25}$$

where the function $B_{_0}$ only depends on the heavy freedoms which are integrated out. In the effective theory, there are two deductions from the WTIs:

- the effective $\bar{s}b\gamma$ (g) vertices can be formulated as

$$\begin{aligned}
iA_{_\mu}^\gamma(p,k) &= \frac{i}{(4\pi)^2} ee_{_d} m_{_b}\Big\{B_{_1}^\gamma\Big(2p_{_\mu} + \not{k}\gamma_{_\mu}\Big) + B_{_2}^\gamma[\not{k}, \gamma_{_\mu}]\Big\}\omega_+ \;, \\
iA_{_\mu}^g(p,k) &= \frac{i}{(4\pi)^2} g_{_s} T^a m_{_b}\Big\{B_{_1}^g\Big(2p_{_\mu} + \not{k}\gamma_{_\mu}\Big) + B_{_2}^g[\not{k}, \gamma_{_\mu}]\Big\}\omega_+
\end{aligned} \tag{26}$$

  after we expand $A_{_\mu}^{\gamma\,(g)}(p,k)$ in powers of the external momenta to the second order, where $B_{_{1,2}}^{\gamma,g}$ are the functions of heavy freedoms only;

- additionally, $B_{_0} = B_{_1}^\gamma = B_{_1}^g$.

The above deductions can be taken as the criterion to test our calculations. In Eq. 26, the functions $B_{_2}^{\gamma,g}$ are proportional to the Wilson coefficients of the magnetic and chromo-magnetic dipole operators respectively.

As an application, we will investigate the CP asymmetry of the rare decay $B \to X_{_s}\gamma$ within the framework of MSSM.

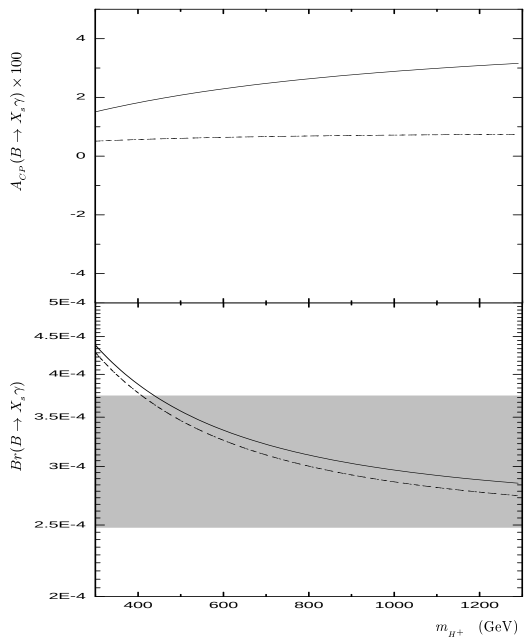

FIG. 4: The CP asymmetry and branching ratio of the inclusive $B \to X_s\gamma$ decay versus the charged Higgs mass m_{H^+}. Dash-line: theoretical prediction at the one-loop order, and solid-line: theoretical prediction at the two-loop order, when $\tan\beta = 30$, $|m_2| = 300$ GeV, $m_{s_R} = 500$ GeV, the other parameters are taken as in the text. The gray band is the experimental allowed region for the branching ratio $BR(B \to X_s\gamma)$ at 1σ deviation.

III. DIRECT CP VIOLATION IN $B \to X_s\gamma$

In the SM, the CP asymmetry of the $B \to X_s\gamma$ process

$$A_{CP}(B \to X_s\gamma) = \frac{\Gamma(\bar{B} \to X_{\bar{s}}\gamma) - \Gamma(B \to X_s\gamma)}{\Gamma(\bar{B} \to X_{\bar{s}}\gamma) + \Gamma(B \to X_s\gamma)} \tag{27}$$

is calculated to be rather small: $A_{CP} \sim 0.5\%$ [15]. For experimental data, the recent measurement [16] of the CP asymmetry implies the 95% range of

$$-0.30 \le A_{CP}(B \to X_s\gamma) \le 0.14\ . \tag{28}$$

In other words, studies of the direct CP asymmetry in $B \to X_s\gamma$ may uncover new sources of the CP violation which lie outside the SM. Up to the NLO, the complete theoretical prediction has been presented in Ref.[17]. In order to eliminate the strong dependence on the b-quark mass, the branching ratios is usually normalized by the decay rate of the B

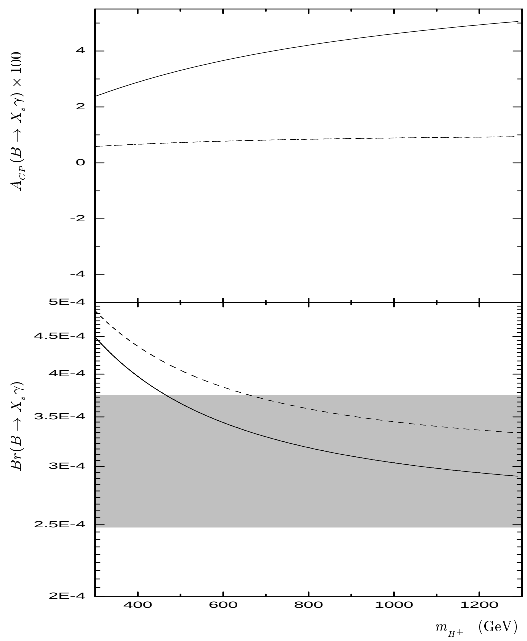

FIG. 5: The CP asymmetry and branching ratio of the inclusive $B \to X_s\gamma$ decay versus the charged Higgs mass m_{H^+}. Dash-line: theoretical prediction at the one-loop order, and solid-line: theoretical prediction at the two-loop order, when $\tan\beta = 60$, $|m_2| = 300$ GeV, $m_{s_R} = 500$ GeV, the other parameters are taken as in the text. The gray band is the experimental allowed region for the branching ratio $BR(B \to X_s\gamma)$ at 1σ deviation.

meson semileptonic decay:

$$\frac{\Gamma(B\to X_s\gamma)}{\Gamma(B\to X_ce\bar{\nu})} = \frac{6\alpha}{\pi f(z)}\Big|\frac{V_{ts}^*V_{tb}}{V_{cb}}C_7(\mu_b)\Big|^2 , \tag{29}$$

where $f(z) = 1 - 8z + 8z^3 - z^4 - 12z^2\ln z$ is the phase-space factor with $z = (m_c/m_b)^2$, and $\alpha = e^2/(4\pi)$ is the electroweak fine-structure constant. The CP asymmetry in the rare decay $B \to X_s\gamma$ is correspondingly formulated as [15]

$$\begin{aligned} A_{CP}(B\to X_s\gamma) = \frac{\alpha_s(\mu_b)}{|C_7(\mu_b)|^2}\Big\{&\frac{40}{81}\mathbf{Im}[C_2(\mu_b)C_7^*(\mu_b)] - \frac{4}{9}\mathbf{Im}[C_8(\mu_b)C_7^*(\mu_b)] \\ &-\frac{8z}{9}g(z)\mathbf{Im}\Big[\Big(1+\frac{V_{us}^*V_{ub}}{V_{ts}^*V_{tb}}\Big)C_2(\mu_b)C_7^*(\mu_b)\Big]\Big\} , \end{aligned} \tag{30}$$

with $g(z) = \Big(5 + \ln z + \ln^2 z - \pi^2/3\Big) + \Big(\ln^2 z - \pi^2/3\Big)z + \Big(28/9 - 4/3\ln z\Big)z^2 + \mathcal{O}(z^3)$. The $C_2(\mu_b)$ is the Wilson coefficient of the operator $\mathcal{O}_2 = \bar{s}_L\gamma_\mu q_L\bar{q}_L\gamma^\mu b_L$ $(q = c,\ u)$ at the hadronic scale. From now on we shall assume the value $BR(B \to X_ce\bar{\nu}) = 10.5\%$ for the

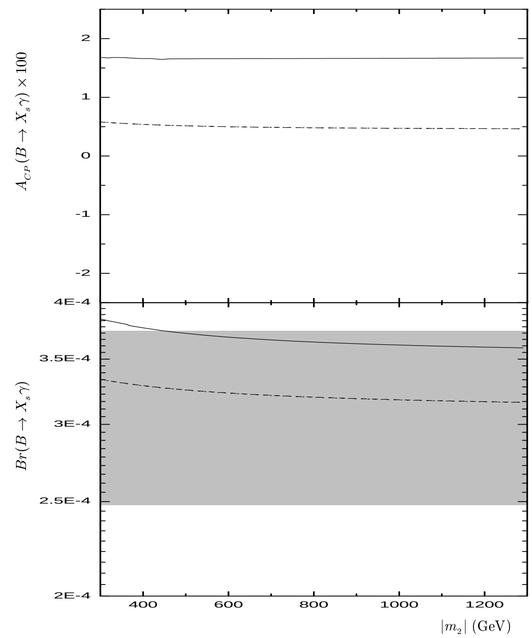

FIG. 6: The CP asymmetry and branching ratio of the inclusive $B \to X_s\gamma$ decay versus the parameter $|m_2|$. Dash-line: theoretical prediction at the one-loop order, and solid-line: theoretical prediction at the two-loop order, when $\tan\beta = 30$, $m_{H^+} = 600$ GeV, $m_{s_R} = 200$ GeV, the other parameters are taken as in the text. The gray band is the experimental allowed region for the branching ratio $BR(B \to X_s\gamma)$ at 1σ deviation.

semileptonic branching ratio, $\alpha_s(m_z) = 0.118$, $\alpha(m_z) = 1/127$. For the standard particle masses, we take $m_t = 174$ GeV, $m_b = 4.2$ GeV, $m_w = 80.42$ GeV, $m_z = 91.19$ GeV and $z = m_c/m_b = 0.29$. In the CKM matrix, we apply the Wolfenstein parameterization and set $A = 0.85$, $\lambda = 0.22$, $\rho = 0.22$, $\eta = 0.35$ [18]. Without loss of generality, we always assume the supersymmetric parameters $\mu = A_t e^{-i\pi/2} = 100$ GeV, $m_3 e^{-i\pi/4} = 300$ GeV, $A_s e^{-i\pi/2} = m_{t_R} = 200$ GeV, $m_{t_L} = m_{s_L} = 5$ TeV here. In order to suppress the one-loop EDMs, we choose the μ parameter CP phase $\theta_\mu = 0$. As for the CP phase which is contained in the $SU(2)$ gaugino mass parameter m_2, it is set as $\theta_2 = arg(m_2) = \pi/4$.

Taking $\tan\beta = 30$, $|m_2| = 300$ GeV, $m_{s_R} = 500$ GeV, we plot the CP asymmetry and branching ratio of the inclusive $B \to X_s\gamma$ decay versus the charged Higgs mass in FIG. 4. Considering the experimental constraint on the branching ratio $BR(B \to X_s\gamma)$ at 1σ tolerance, the CP asymmetry including the two-loop corrections can be larger than 3%, and the one-loop result is smaller than 1% with our chosen parameters. The choice of parameter

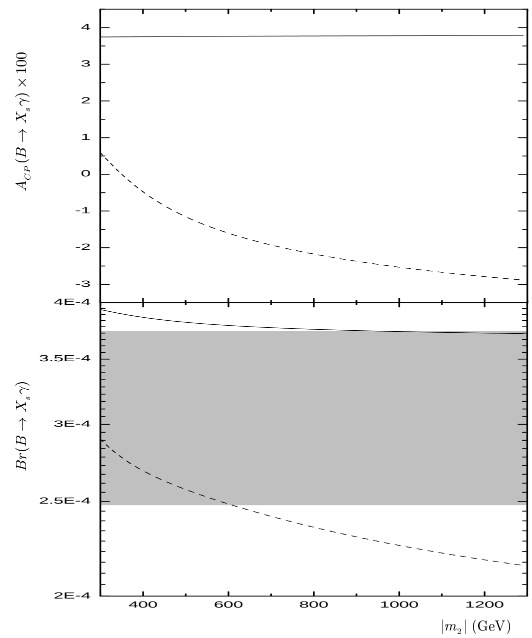

FIG. 7: The CP asymmetry and branching ratio of the inclusive $B \to X_s\gamma$ decay versus the parameter $|m_2|$. Dash-line: theoretical prediction at the one-loop order, and solid-line: theoretical prediction at the two-loop order, when $\tan\beta = 60$, $m_{H^+} = 600$ GeV, $m_{s_R} = 200$ GeV, the other parameters are taken as in the text. The gray band is the experimental allowed region for the branching ratio $BR(B \to X_s\gamma)$ at 1σ deviation.

space of FIG. 5 is identical with that of FIG. 4 except for $\tan\beta = 60$. After including the two-loop corrections, we find that the CP asymmetry can reach 5% with an increasing of the charged Higgs mass when $\tan\beta = 60$, while at the same time keeping the branching ratio $BR(B \to X_s\gamma)$ is within the 1σ deviation experimental bound. Since the two-loop correction is proportional to $\tan\beta$, we can understand why the differences between the one- and two-loop predictions of FIG. 5 ($\tan\beta = 60$) are larger than that of FIG. 4 ($\tan\beta = 30$). From the numerical analysis, we find that the two-loop corrections to the Wilson coefficients are still rather smaller than the one-loop results at $\tan\beta = 30$, while the two-loop corrections are comparable with the one-loop results at $\tan\beta = 60$. Since the bottom quark Yukawa coupling approximates to 1 at $\tan\beta = 60$, it should be argued whether or not we can safely apply the perturbative expansion to give the theoretical predictions of physics observables for such high $\tan\beta$.

Now, let us study the variance of two-loop results with the soft $SU(2)$ gaugino mass

parameter $|m_2|$. Taking $\tan\beta = 30$, $m_{s_R} = 200$ GeV, $m_{H^+} = 600$ GeV, we plot the theoretical predictions for the CP asymmetry and branching ratio of the inclusive $B \to X_s\gamma$ decay versus the parameter $|m_2|$ in FIG. 6 at one- and two-loop order respectively. If the theoretical prediction for the branching ratio satisfies with the experimental bound at 1σ deviation

$$2.48 \times 10^{-4} \leq BR(B \to X_s\gamma) \leq 3.74 \times 10^{-4} \ ,$$

the CP asymmetry including the two-loop corrections is about $\sim 1.5\%$. The choice of the parameter space in FIG. 7 is identical with that of FIG. 6 except for $\tan\beta = 60$. In this scenario, the two-loop prediction on the asymmetry is about $\sim 4\%$. Note that the dependence of the two-loop corrections on the parameter $|m_2|$ is milder than that on the charged Higgs mass m_{H^+}. This fact can be understood as follows: the amplitudes of the corresponding triangle diagrams depend on the charged Higgs mass in form $1/(Q^2 - m_{H^+}^2)$ (Q denotes loop momenta q_1, q_2, or or $q_2 - q_1$), and depend on the parameter $|m_2|$ through the chargino propagator $(\not{Q} - m_\chi)/(Q^2 - m_\chi^2)$ (m_χ denotes the chargino mass) before the loop momentum integration.

In our analysis, we do not compare the exact two-loop analysis with the HME result since the discussion has already been presented in Ref. [10].

IV. CONCLUSIONS

In this work, we present the complete two-loop gluino corrections to inclusive $B \to X_s\gamma$ decay in explicit CP violating MSSM within large $\tan\beta$ scenarios. Beside the diagrams where quark flavor change is mediated by the charged Higgs, we also include those diagrams in which quark flavor change is mediated by the charginos. Using loop momentum translation invariant, we formulate our expressions fulfilling the $SU(3)_c \times U(1)_{em}$ WTIs. From the numerical analysis, we show that the two-loop corrections to the branching ratio are comparable with the one-loop predictions at large $\tan\beta$. Correspondingly, the CP asymmetry can also reach about 5%, which is much larger than that predicted by the SM.

Acknowledgments

The work has been supported by the Academy of Finland under the contract no. 104915.

APPENDIX A: IDENTITIES AMONG THE TWO-LOOP SCALAR INTEGRALS

Here, we report the identities that are used in the process of obtaining Eq. 18 and Eq.19, they can be derived from the loop momentum translation invariant of the amplitudes. They are

$$\int \frac{d^D q_1}{(2\pi)^D}\frac{d^D q_2}{(2\pi)^D}\frac{1}{\mathcal{D}_0}\Big\{\frac{q_1^2 q_1\cdot(q_2-q_1)}{(q_2-q_1)^2-m_0^2}+\frac{q_1^2 q_1\cdot q_2}{q_2^2-m_\alpha^2}\Big\}\equiv 0\;,$$

$$\int \frac{d^D q_1}{(2\pi)^D}\frac{d^D q_2}{(2\pi)^D}\frac{1}{\mathcal{D}_0}\Big\{\frac{2}{(q_2-q_1)^2-m_0^2}\frac{(q_1\cdot q_2)^2-q_1^2q_2^2}{D(D-1)}+\frac{q_1\cdot q_2}{D}\Big\}\equiv 0\;,$$

$$\int \frac{d^D q_1}{(2\pi)^D}\frac{d^D q_2}{(2\pi)^D}\frac{1}{\mathcal{D}_0}\Big\{-\frac{q_1\cdot(q_2-q_1)}{D}+\frac{2}{q_2^2-m_\alpha^2}\frac{(q_1\cdot q_2)^2-q_1^2q_2^2}{D(D-1)}\Big\}\equiv 0\;,$$

$$\int \frac{d^D q_1}{(2\pi)^D}\frac{d^D q_2}{(2\pi)^D}\frac{1}{\mathcal{D}_0}\Big\{\frac{1}{(q_2-q_1)^2-m_0^2}\Big[\frac{D(q_1\cdot q_2)^2-q_1^2q_2^2}{D(D-1)}-\frac{q_1^2 q_1\cdot q_2}{D}\Big]$$
$$+\frac{1}{q_2^2-m_\alpha^2}\frac{D(q_1\cdot q_2)^2-q_1^2q_2^2}{D(D-1)}\Big\}\equiv 0\;,$$

$$\int \frac{d^D q_1}{(2\pi)^D}\frac{d^D q_2}{(2\pi)^D}\frac{1}{\mathcal{D}_0}\Big\{-q_1^2+\frac{2}{D}\frac{q_1^2 q_2\cdot(q_2-q_1)}{(q_2-q_1)^2-m_0^2}+\frac{2}{D}\frac{q_1^2q_2^2}{q_2^2-m_\alpha^2}\Big\}\equiv 0\;,$$

$$\int \frac{d^D q_1}{(2\pi)^D}\frac{d^D q_2}{(2\pi)^D}\frac{1}{\mathcal{D}_0}\Big\{-q_1\cdot q_2+\frac{q_2^2 q_1\cdot(q_2-q_1)}{(q_2-q_1)^2-m_0^2}+\frac{q_2^2 q_1\cdot q_1}{q_2^2-m_\alpha^2}\Big\}\equiv 0\;,$$

$$\int \frac{d^D q_1}{(2\pi)^D}\frac{d^D q_2}{(2\pi)^D}\frac{1}{\mathcal{D}_0}\Big\{-\frac{2+D}{2}q_2^2+\frac{q_2^2 q_2\cdot(q_2-q_1)}{(q_2-q_1)^2-m_0^2}+\frac{q_2^4}{q_2^2-m_\alpha^2}\Big\}\equiv 0\;,$$

$$\int \frac{d^D q_1}{(2\pi)^D}\frac{d^D q_2}{(2\pi)^D}\frac{1}{\mathcal{D}_0}\Big\{-q_1\cdot q_2+\frac{2}{(q_2-q_1)^2-m_0^2}\frac{q_1\cdot q_2(q_2-q_1)^2}{D}$$
$$+\frac{2}{q_2^2-m_\alpha^2}\Big[\frac{q_1\cdot q_2 q_2^2}{D}-\frac{D(q_1\cdot q_2)^2-q_1^2q_2^2}{D(D-1)}\Big]\Big\}\equiv 0\;,$$

$$\int \frac{d^D q_1}{(2\pi)^D}\frac{d^D q_2}{(2\pi)^D}\frac{1}{\mathcal{D}_0}\Big\{\frac{1}{(q_2-q_1)^2-m_0^2}\Big[q_1\cdot q_2 q_2\cdot(q_2-q_1)-\frac{D+1}{2}q_2^2 q_1\cdot(q_2-q_1)\Big]$$
$$-\frac{D-1}{2}\frac{q_2^2 q_1\cdot q_2}{q_2^2-m_\alpha^2}\Big\}\equiv 0\;,$$

$$\int \frac{d^D q_1}{(2\pi)^D}\frac{d^D q_2}{(2\pi)^D}\frac{1}{\mathcal{D}_0}\Big\{\frac{2}{D}\frac{q_2\cdot(q_2-q_1)}{(q_2-q_1)^2-m_0^2}+\frac{2}{D}\frac{q_2^2}{q_2^2-m_\alpha^2}-1\Big\}\equiv 0\;,$$

$$\int \frac{d^D q_1}{(2\pi)^D}\frac{d^D q_2}{(2\pi)^D}\frac{1}{\mathcal{D}_0}\Big\{\frac{2}{D}\frac{(q_2-q_1)^2}{(q_2-q_1)^2-m_0^2}+\frac{2}{D}\frac{q_2\cdot(q_2-q_1)}{q_2^2-m_\alpha^2}-1\Big\}\equiv 0\;,$$

$$\int \frac{d^D q_1}{(2\pi)^D}\frac{d^D q_2}{(2\pi)^D}\frac{1}{\mathcal{D}_0}\Big\{\frac{q_1\cdot(q_2-q_1)}{D}-\frac{2}{q_2^2-m_\alpha^2}\frac{(q_1\cdot q_2)^2-q_1^2q_2^2}{D(D-1)}\Big\}\equiv 0\;,$$

$$\int \frac{d^Dq_1}{(2\pi)^D}\frac{d^Dq_2}{(2\pi)^D}\frac{1}{\mathcal{D}_0}\Big\{\frac{q_2\cdot(q_2-q_1)}{D}+\frac{2}{q_1^2-m_a^2}\frac{(q_1\cdot q_2)^2-q_1^2q_2^2}{D(D-1)}\Big\}\equiv 0\;,$$
$$\int \frac{d^Dq_1}{(2\pi)^D}\frac{d^Dq_2}{(2\pi)^D}\frac{1}{\mathcal{D}_0}\Big\{-\frac{2+D}{D}q_1\cdot q_2+\frac{2}{q_1^2-m_a^2}\frac{q_1^2q_1\cdot q_2}{D}$$
$$+\frac{2}{q_2^2-m_\alpha^2}\frac{D(q_1\cdot q_2)^2-q_1^2q_2^2}{D(D-1)}\Big\}\equiv 0\;,$$
$$\int \frac{d^Dq_1}{(2\pi)^D}\frac{d^Dq_2}{(2\pi)^D}\frac{1}{\mathcal{D}_0}\Big\{-\frac{2+D}{D}q_1\cdot q_2+\frac{2}{q_1^2-m_a^2}\frac{D(q_1\cdot q_2)^2-q_1^2q_2^2}{D(D-1)}$$
$$+\frac{2}{q_2^2-m_\alpha^2}\frac{q_1\cdot q_2q_2^2}{D}\Big\}\equiv 0\;,$$
$$\int \frac{d^Dq_1}{(2\pi)^D}\frac{d^Dq_2}{(2\pi)^D}\frac{1}{\mathcal{D}_0}\Big\{-\frac{2+D}{2}q_1^2+\frac{q_1^4}{q_1^2-m_a^2}+\frac{q_1^2q_1\cdot q_2}{q_2^2-m_\alpha^2}\Big\}\equiv 0\;,$$
$$\int \frac{d^Dq_1}{(2\pi)^D}\frac{d^Dq_2}{(2\pi)^D}\frac{1}{\mathcal{D}_0}\Big\{-\frac{2+D}{2}q_2^2+\frac{q_1\cdot q_2q_2^2}{q_1^2-m_a^2}+\frac{q_2^4}{q_2^2-m_\alpha^2}\Big\}\equiv 0\;,$$
$$\int \frac{d^Dq_1}{(2\pi)^D}\frac{d^Dq_2}{(2\pi)^D}\frac{1}{\mathcal{D}_0}\Big\{-q_2\cdot(q_2-q_1)+\frac{q_1\cdot(q_2-q_1)q_2^2}{q_1^2-m_a^2}+\frac{q_2\cdot(q_2-q_1)q_2^2}{q_2^2-m_\alpha^2}\Big\}\equiv 0\;,$$
$$\int \frac{d^Dq_1}{(2\pi)^D}\frac{d^Dq_2}{(2\pi)^D}\frac{1}{\mathcal{D}_0}\Big\{\frac{2}{D}\frac{q_1^2}{q_1^2-m_a^2}+\frac{2}{D}\frac{q_1\cdot q_2}{q_2^2-m_\alpha^2}-1\Big\}\equiv 0\;,$$
$$\int \frac{d^Dq_1}{(2\pi)^D}\frac{d^Dq_2}{(2\pi)^D}\frac{1}{\mathcal{D}_0}\Big\{\frac{2}{D}\frac{q_1\cdot q_2}{q_1^2-m_a^2}+\frac{2}{D}\frac{q_2^2}{q_2^2-m_\alpha^2}-1\Big\}\equiv 0\;, \tag{A1}$$

with $\mathcal{D}_0=((q_2-q_1)^2-m_0^2)(q_1^2-m_a^2)(q_2^2-m_\alpha^2)$, and D is the time-space dimension. In addition the two-loop vacuum integral

$$\int \frac{d^Dq_1}{(2\pi)^D}\frac{d^Dq_2}{(2\pi)^D}\frac{1}{\mathcal{D}_0}, \tag{A2}$$

has been discussed in Ref. [14].

APPENDIX B: FORM FACTORS IN THE TWO-LOOP WILSON COEFFICIENTS

$$\mathcal{N}^\gamma_{H(1)}=-\frac{q_1^2q_1\cdot q_2}{(q_1^2-m_{\tilde{s}_i}^2)^2}-\frac{1}{3}\frac{4(q_1\cdot q_2)^2-q_1^2q_2^2}{(q_1^2-m_{\tilde{s}_i}^2)(q_2^2-m_{H^+}^2)}-\frac{q_1\cdot q_2q_2^2}{(q_2^2-m_{H^+}^2)^2}$$
$$+\frac{q_1\cdot q_2}{q_1^2-m_{\tilde{s}_i}^2}+\frac{q_1\cdot q_2}{q_2^2-m_t^2}\;,$$
$$\mathcal{N}^\gamma_{H(2)}=-\frac{q_1^2}{(q_1^2-m_{\tilde{s}_i}^2)^2}-\frac{q_1\cdot q_2}{(q_1^2-m_{\tilde{s}_i}^2)(q_2^2-m_{H^+}^2)}-\frac{q_2^2}{(q_2^2-m_{H^+}^2)^2}+\frac{1}{q_1^2-m_{\tilde{s}_i}^2}$$

$$+\frac{1}{q_2^2-m^2_{_{H^+}}}+\frac{2}{q_2^2-m^2_{_t}}\Big]\;,$$

$$\mathcal{N}^g_{_{H(1)}}=-\frac{q_1^2q_1\cdot q_2}{(q_1^2-m^2_{_{\tilde{s}_i}})^2}-\frac{1}{3}\frac{4(q_1\cdot q_2)^2-q_1^2q_2^2}{(q_1^2-m^2_{_{\tilde{s}_i}})(q_2^2-m^2_{_{H^+}})}-\frac{q_1\cdot q_2q_2^2}{(q_2^2-m^2_{_{H^+}})^2}+\frac{17}{8}\frac{q_1\cdot q_2}{q_1^2-m^2_{_{\tilde{s}_i}}}$$
$$-\frac{1}{16}\frac{8q_1\cdot q_2-9q_2^2}{q_2^2-m^2_{_t}}+\frac{3}{16}\frac{8q_1\cdot q_2+3q_2^2}{q_2^2-m^2_{_{H^+}}}-\frac{9}{16}\;,$$

$$\mathcal{N}^g_{_{H(2)}}=-\frac{q_1^2}{(q_1^2-m^2_{_{\tilde{s}_i}})^2}-\frac{q_1\cdot q_2}{(q_1^2-m^2_{_{\tilde{s}_i}})(q_2^2-m^2_{_{H^+}})}-\frac{q_2^2}{(q_2^2-m^2_{_{H^+}})^2}+\frac{1}{q_1^2-m^2_{_{\tilde{s}_i}}}$$
$$+\frac{1}{q_2^2-m^2_{_{H^+}}}-\frac{1}{q_2^2-m^2_{_t}}-\frac{9}{8}\frac{1}{q_1^2-|m_{_3}|^2}\;,$$

$$\mathcal{N}^\gamma_{_{\chi_k^\pm(1)}}=\frac{q_1^2q_1\cdot(q_2-q_1)}{(q_1^2-m^2_{_{\tilde{s}_i}})^2}-\frac{1}{3}\frac{3q_1^2q_1\cdot q_2-4(q_1\cdot q_2)^2+q_1^2q_2^2}{(q_1^2-m^2_{_{\tilde{s}_i}})(q_2^2-m^2_{_{\chi_k}})}+\frac{q_1\cdot(q_2-q_1)q_2^2}{(q_2^2-m^2_{_{\chi_k}})^2}$$
$$-\frac{q_1\cdot(q_2-q_1)}{q_2^2-m^2_{_{\tilde{t}_j}}}-\frac{2q_1^2-q_1\cdot q_2}{q_2^2-m^2_{_{\chi_k}}}-\frac{q_1\cdot q_2}{q_2^2-m^2_{_{\tilde{t}_j}}}\;,$$

$$\mathcal{N}^\gamma_{_{\chi_k^\pm(2)}}=\frac{q_1^2q_1\cdot q_2}{(q_1^2-m^2_{_{\tilde{s}_i}})^2}-\frac{1}{3}\frac{4(q_1\cdot q_2)^2-q_1^2q_2^2}{(q_1^2-m^2_{_{\tilde{s}_i}})(q_2^2-m^2_{_{\chi_k}})}+\frac{q_1\cdot q_2q_2^2}{(q_2^2-m^2_{_{\chi_k}})^2}$$
$$-\frac{q_1\cdot q_2}{q_1^2-m^2_{_{\tilde{s}_i}}}-\frac{q_1\cdot q_2}{q_2^2-m^2_{_{\tilde{t}_j}}}\;,$$

$$\mathcal{N}^\gamma_{_{\chi_k^\pm(3)}}=\frac{q_1^2q_2\cdot(q_2-q_1)}{(q_1^2-m^2_{_{\tilde{s}_i}})^2}+\frac{1}{3}\frac{3q_1\cdot q_2q_2^2-4(q_1\cdot q_2)^2+q_1^2q_2^2}{(q_1^2-m^2_{_{\tilde{s}_i}})(q_2^2-m^2_{_{\chi_k}})}+\frac{q_2\cdot(q_2-q_1)q_2^2}{(q_2^2-m^2_{_{\chi_k}})^2}$$
$$-\frac{q_2\cdot(q_2-q_1)}{q_1^2-m^2_{_{\tilde{s}_i}}}-\frac{q_2^2}{q_2^2-m^2_{_{\chi_k}}}-\frac{2q_2^2-q_1\cdot q_2}{q_2^2-m^2_{_{\tilde{t}_j}}}-2\;,$$

$$\mathcal{N}^\gamma_{_{\chi_k^\pm(4)}}=-\frac{q_1^2}{(q_1^2-m^2_{_{\tilde{s}_i}})^2}-\frac{q_2^2}{(q_2^2-m^2_{_{\chi_k}})^2}-\frac{q_1\cdot q_2}{(q_1^2-m^2_{_{\tilde{s}_i}})(q_2^2-m^2_{_{\chi_k}})}$$
$$+\frac{1}{q_1^2-m^2_{_{\tilde{s}_i}}}-\frac{2}{q_2^2-m^2_{_{\chi_k}}}-\frac{2}{(q_2-q_1)^2-m^2_{_t}}\;,$$

$$\mathcal{N}^g_{_{\chi_k^\pm(1)}}=\frac{q_1^2q_1\cdot(q_2-q_1)}{(q_1^2-m^2_{_{\tilde{s}_i}})^2}-\frac{1}{3}\frac{3q_1^2q_1\cdot q_2-4(q_1\cdot q_2)^2+q_1^2q_2^2}{(q_1^2-m^2_{_{\tilde{s}_i}})(q_2^2-m^2_{_{\chi_k}})}+\frac{q_1\cdot(q_2-q_1)q_2^2}{(q_2^2-m^2_{_{\chi_k}})^2}$$
$$-\frac{17}{8}\frac{q_1\cdot(q_2-q_1)}{q_1^2-m^2_{_{\tilde{s}_i}}}-\frac{1}{16}\frac{7q_1\cdot q_2-q_1^2+9q_2^2}{q_2^2-m^2_{_{\chi_k}}}-\frac{9}{16}\frac{q_2\cdot(q_2-q_1)}{q_2^2-m^2_{_{\tilde{t}_j}}}\;,$$

$$\mathcal{N}^g_{_{\chi_k^\pm(2)}}=\frac{q_1^2q_1\cdot q_2}{(q_1^2-m^2_{_{\tilde{s}_i}})^2}+\frac{1}{3}\frac{4(q_1\cdot q_2)^2-q_1^2q_2^2}{(q_1^2-m^2_{_{\tilde{s}_i}})(q_2^2-m^2_{_{\chi_k}})}+\frac{q_1\cdot q_2q_2^2}{(q_2^2-m^2_{_{\chi_k}})^2}$$
$$-\frac{17}{8}\frac{q_1\cdot q_2}{q_1^2-m^2_{_{\tilde{s}_i}}}-\frac{3}{16}\frac{8q_1\cdot q_2+3q_2^2}{q_2^2-m^2_{_{\chi_k}}}+\frac{1}{16}\frac{8q_1\cdot q_2-9q_2^2}{q_2^2-m^2_{_{\tilde{t}_j}}}+\frac{9}{8}\;,$$

$$\mathcal{N}^g_{_{\chi_k^\pm(3)}}=\frac{q_1^2q_2\cdot(q_2-q_1)}{(q_1^2-m^2_{_{\tilde{s}_i}})^2}+\frac{1}{3}\frac{3q_1\cdot q_2q_2^2-4(q_1\cdot q_2)^2+q_1^2q_2^2}{(q_1^2-m^2_{_{\tilde{s}_i}})(q_2^2-m^2_{_{\chi_k}})}+\frac{q_2\cdot(q_2-q_1)q_2^2}{(q_2^2-m^2_{_{\chi_k}})^2}$$

$$
-\frac{q_2\cdot(q_2-q_1)}{q_1^2-m_{\tilde{s}_i}^2}+\frac{1}{8}\frac{12q_1\cdot q_2-13q_2^2}{q_2^2-m_{\chi_k}^2}+\frac{1}{16}\frac{7q_2^2-8q_1\cdot q_2}{q_2^2-m_{\tilde{t}_j}^2}+\frac{9}{8}\frac{q_2\cdot(q_2-q_1)}{q_1^2-|m_3|^2}+\frac{1}{8}\,,
$$

$$
\begin{aligned}
\mathcal{N}^g_{\chi_k^\pm(4)} &= -\frac{q_1^2}{(q_1^2-m_{\tilde{s}_i}^2)^2}-\frac{q_1\cdot q_2}{(q_1^2-m_{\tilde{s}_i}^2)(q_2^2-m_{\chi_k}^2)}+\frac{q_2^2}{(q_2^2-m_{\chi_k}^2)^2}+\frac{1}{q_1^2-m_{\tilde{s}_i}^2}\\
&+\frac{1}{q_2^2-m_{\chi_k}^2}-\frac{9}{8}\frac{1}{q_1^2-|m_3|^2}-\frac{1}{8}\frac{1}{(q_2-q_1)^2-m_t^2}\,. \qquad \text{(B1)}
\end{aligned}
$$

[1] K. Abe *et al.* [BELLE Collaboration], Phys. Lett. B **511**, 151(2001); S. Chen *et al.* [CLEO Collaboration], Phys. Rev. Lett. **87**, 251807(2001); B. Aubert *et al.* [BABAR Collaboration], hep-ex/0207074, hep-ex/0207076.

[2] K. Chetyrkin, M. Misiak, and M. Munz, Phys. Lett. B **400**, 206(1997); *ibid.* **425**, 414(1997)(E); T. Hurth, hep-ph/0106050; C. Greub, T. Hurth, and D. Wyler, Phys. Rev. D **54**, 3350(1996); K. Adel and Y. Yao, *ibid.* **49**, 4945(1994); A. Ali and C. Greub, Phys. Lett. B **361**, 146(1995).

[3] A. Pilaftsis, Phys. Lett. B **435**, 88(1998); D. A. Demir, Phys. Rev. D **60**, 055006(1999); A. Pilaftsis and C. E. Wagner, Nucl. Phys. B **553**, 3(1999); T. Ibrahim and P. Nath, Phys. Rev. D **63**, 035009(2001); M. Carena, J. Ellis, A. Pilaftsis, and C. E. Wagner, Nucl. Phys. B **586**, 92(2000); Phys. Lett. B **495**, 155(2000).

[4] T. Ibrahim, P. Nath, Phys. Lett. B **418**, 98(1998); Phys. Rev. D **57**, 478(1998); **58**, 111301(1998); **61**, 093004(2000); M. Brhlik, G. J. Good, G. L. Kane, *ibid.* **59**, 115004(1999); A. Bartl, T. Gajdosik, W. Porod, P. Stockinger and H. Stremnitzer, *ibid.* **60**, 073003(1999).

[5] P. Nath, Phys. Rev. Lett. **66**, 2565(1991); Y. Kizukuri and N. Oshimo, Phys. Rev. D. **45**, 1806(1992); **46**, 3025(1992); D. Chang, W. Keung and A. Pilaftsis, Phys. Rev. Lett. **82**, 900(1999); A. Pilaftsis, Phys. Lett. B **471**, 174(1999); D. Chang, W. Chang and W. Keung, *ibid.* **478**, 239(2000); T. F. Feng, T. Huang, X. Q. Li, X. M. Zhang, and S. M. Zhao, Phys. Rev. D. **68**, 016004(2003).

[6] F. Kruger and J. C. Romao, Phys. Rev. D **62**, 034020(2000); T. M. Aliev, D. A. Demir, and M. Savci, *ibid.* **62**, 074016(2000).

[7] D. A. Demir and M. B. Voloshin, Phys. Rev. D **63**, 115011(2001).

[8] A. Ali, H. Asatrian, and C. Greub, Phys. Lett. B **429**, 87(1998); A. Ali and E. Lunghi, Eur. Phys. J C **21**, 683(2001); T. Nihei, Prog. Theor. Phys. **98**, 1157(1997); S. Baek and P. Ko, Phys. Rev. Lett. **83**, 488(1999); D. A. Demir, A. Masiero, and O. Vives, *ibid.* **82**, 2447(1999);

S. Baek, Phys. Rev. D **67**, 096004(2003); A. Dedes and A. Pilaftsis, *ibid.* **67**, 015012(2003).

[9] H. Georgi, in "Proceedings of the American Institute of Physics", C. E. Carlson (Ed.), New York, 575(1975); H. Georgi and D. V. Nanopoulos, Nucl. Phys. B **155**, 52(1979); **159**, 16(1979); L. E. Ibáñez and G. R. Ross, Phys. Lett. B **105**, 439(1981); M. Olechowski and S. Pokorski, *ibid.* **214**, 393(1988); D. A. Demir and K. A. Olive, Phys. Rev. D **65**, 034007(2002).

[10] F. Borzumati, C. Greub, and Y. Yamada, Phys. Rev. D **69**, 055005(2004).

[11] G. Degrassi, P. Gambino, and G. F. Giudice, J. High Energy Phys. **12**, 009(2000); M. Carena, D. Garcia, U. Nierste, and C. E. M. Wagner, Phys. Lett. B **499**, 141(2001).

[12] K. Chetyrkin, M. Misiak, and M. Munz, Phys. Lett. B **400**, 206(1997); **425**, 414(E)(1997); T. Hurth, hep-ph/0106050; C. Greub, T. Hurth, and D. Wyler, Phys. Rev. D **54**, 3350(1996); K. Adel and Y. Yao, *ibid.* **49**, 4945(1994); A. Ali and C. Greub, Phys. Lett. B **361**, 146(1995).

[13] For a review, see P. Nath, R. Arnowitt, and A. H. Chamseddine, Applied N=1 supergravity, Lecture series, 1983(World Scientific, Singapore, 1984); H. P. Nilles, Phys. Rep. **110**, 1(1984).

[14] A. I. Davydychev and J. B. Tausk, Nucl. Phys. B **397**, 123(1993).

[15] A. L. Kagan and M. Neubert, Phys. Rev. D **58**, 094012(1998).

[16] CLEO Collaboration, T. E. Coan *et al.*, Phys. Rev. Lett. **86**, 5661(2001).

[17] K. Chetyrkin, M. Misiak, and M. Münz, Phys. Lett. B **400**, 206(1997); **425**, 414(1998)(E).

[18] K. Hagiwara *et al.*, Phys. Rev. D **66**, 010001(2002).